UNIVERSITÀ
DEGLI STUDI DI TRIESTE

INFN

Synthetic life in extreme conditions

Federico Dogo[1,2], Sabrina Stella[1,2]
Roberto Chignola[3] and Edoardo Milotti[1,2],

[1]Dipartimento di Fisica, Università di Trieste
[2]INFN – Sezione di Trieste, Trieste, Italy
[3]Dipartimento di Biotecnologia, Università di Verona, Verona, Italy

Prokaryotes and eukaryotes as paradigms of life

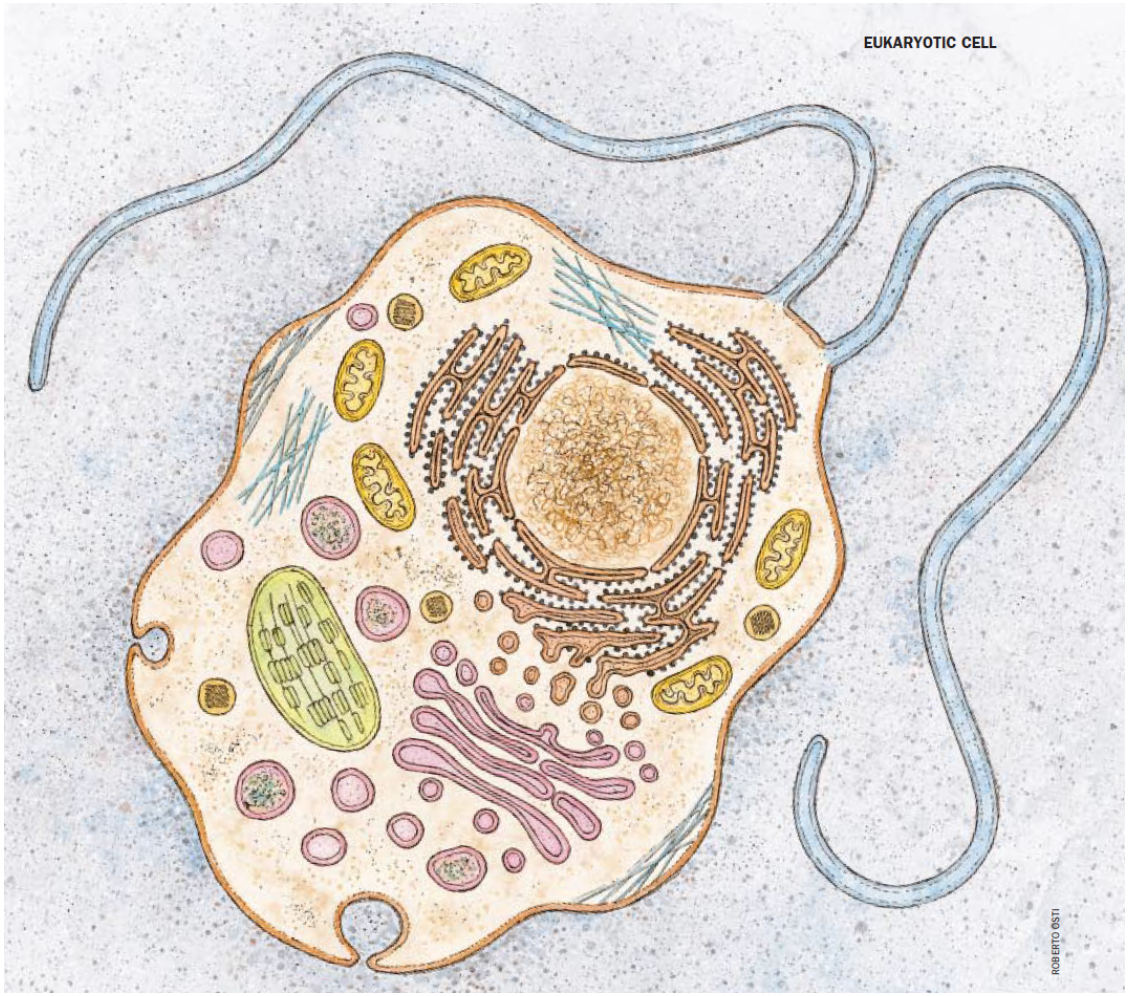

The starting point: tumor spheroids, an *in vitro* model of solid tumors

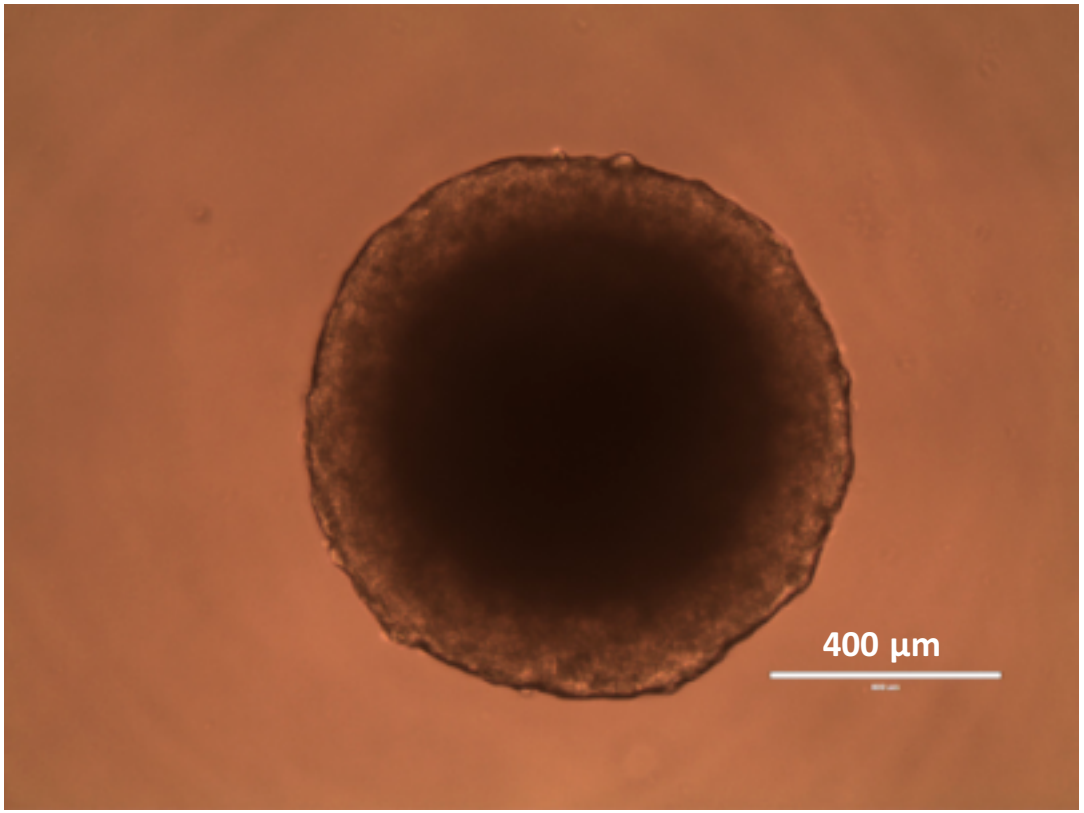

- ✓ Gradient of proliferation
- ✓ Gradient of nutrients, oxygen and pH
- ✓ Intercellular matrix production
- ✓ Expression of adhesion molecules
- ✓ Expression of specific genes
- ✓ Drug resistance
- ✓ Growth kinetics
- ✓ No blood vessels
- ✓ No surrounding tissues

A computational model of tumor spheroids

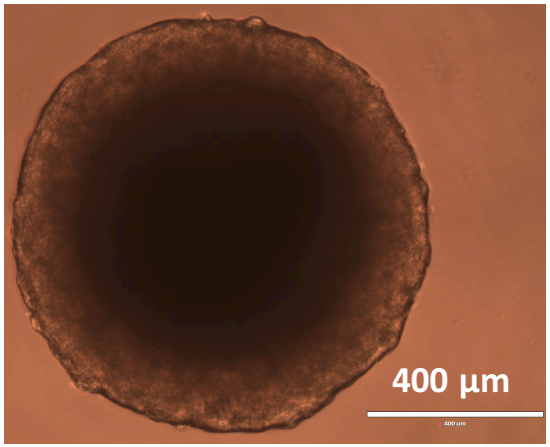

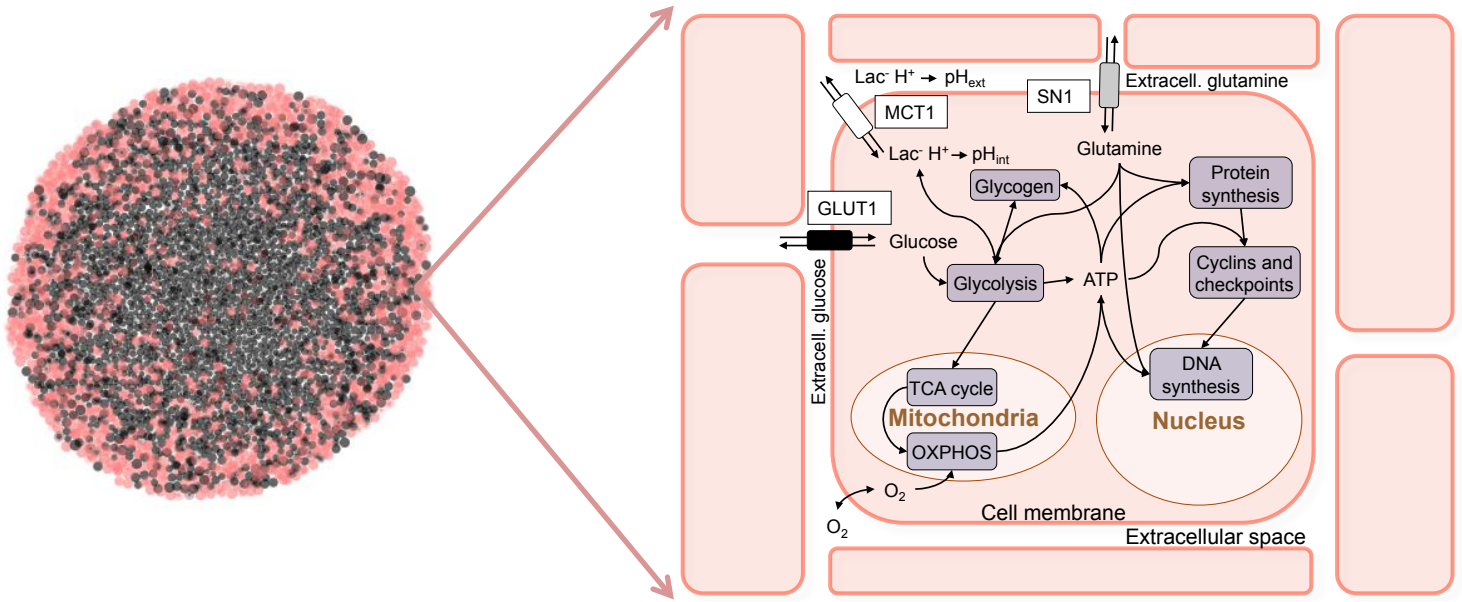

Computational implementation

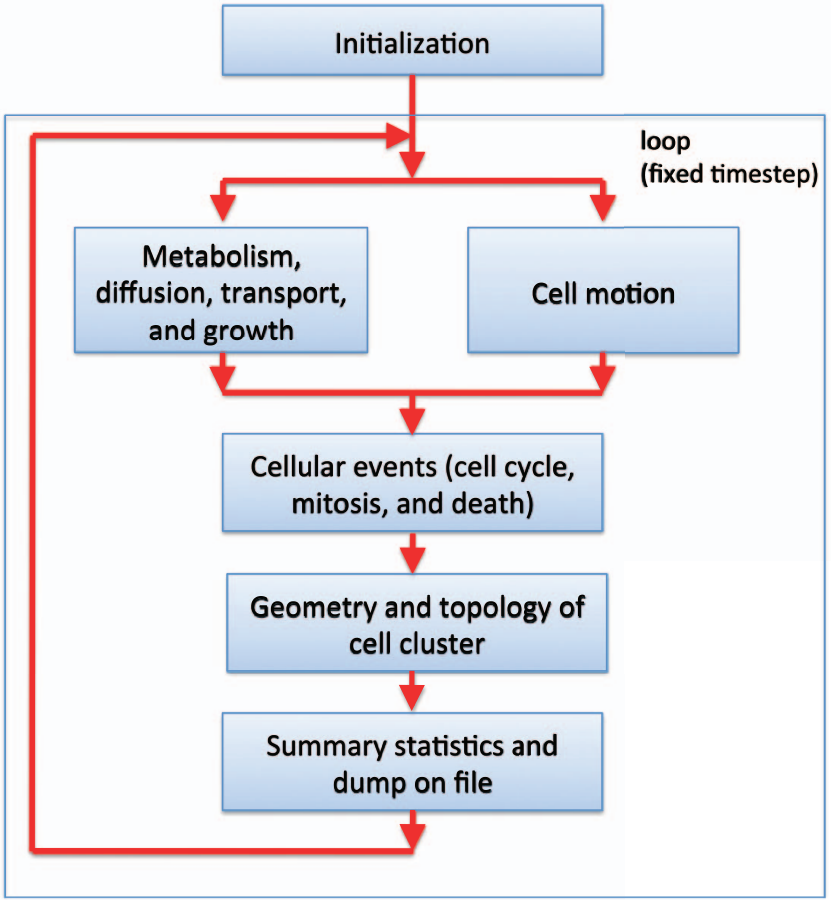

FIG. 1. Block diagram of the simulation program, reproduced from Ref. 12.

This model of human (tumor) cells is unique in its scope, as it includes both the internal biochemical processes and the biomechanics of cells.

We use it to simulate both disperse cells and cell aggregates.

Selected refs.:

R. Chignola, E. Milotti. *AIP Adv.* (2012) **2**: 011204
R. Chignola et al. *J. Bioinf. Comput. Biol.* (2011) **9**: 559
E. Milotti, R. Chignola. *PLoS ONE* (2010) **5**: e13942
E. Milotti et al. Comp. *Phys. Commun.* (2009) **180**: 2166
R. Chignola et al. *Phys. Biol.* (2007) **4**: 114
R. Chignola, E. Milotti. *Phys. Biol.* (2005) **2**: 8
R. Chignola, E. Milotti. *Physica A* (2004) **338**: 261

http://vbl.ts.infn.it/SiteVBL/

Model outputs compare favorably with real data (1)

Table 1. Estimated morphologic, kinetic, and metabolic parameters for a population of dispersed tumor cells and comparison with actual experimental data.

Parameter	Simulated			Experimental	Reference
Morphologic	*Average*	*Min*	*Max*		
Radius (μm)	5.0	4.8	5.3	5.5–7.1	38
Volume (μm^3)	530	471	623	700–1500	38, 39
Mitochondria/cell	220.4	190.6	266.9	83–677[a]	40
Kinetic					
Growth rate[b] (h^{-1})	0.035			0.03–0.035[c]	22
Doubling time[b] (h)	19.8			19.7–22.8[c]	22
G1 (%)	52.5	48.4	59.3	54.4 ± 2.2[c]	21
S (%)	34.5	30.5	40.5	27.5 ± 5.8[c]	21
G2/M (%)	12.9	7.3	17.7	16.4 ± 1.7[c]	21
Metabolic					
ATP/cell[d]	5.5	5.4	5.6	4.3–5.8	21
Glucose uptake[e]	1.9 ± 0.3			2.5 ± 0.2	41
Lactate production[e]	3.8 ± 0.3			3.9 ± 0.8	41
ATP production[e,f]	19.8 ± 8.3			37.8	41
ATP production[e,g]	10.6 ± 1.3			11.4 ± 2.3	41
Oxygen consumption[e]	0.25 ± 0.1			0.48 ± 0.1	41

Notes: [a]Range of the number of mitochondria observed in different cell types.
[b]The growth rate for both simulated and experimental cell populations was calculated by exponential fitting of growth curves. The doubling time was then calculated as log 2/(growth rate).
[c]Data measured for MOLT3 (human T lymphoblastoid cell line) and Raji (human B lymphoblastoid cell line) cells in our own experiments.
[d]Values are expressed as 10^{-18} kg.
[e]Values are expressed as 10^{-19} kg s^{-1}.
[f]ATP production through oxidative phosphorylation.
[g]ATP production through glycolysis.

R. Chignola, A. Del Fabbro, M. Farina, E. Milotti. *J. Bioinf. Comput. Biol.* (2011) **4**: 559

Model outputs compare with actual data (2)

Table 2. Estimated metabolic, histologic, and kinetic, parameters for a virtual multicell tumor spheroid and comparison with actual experimental data.

Parameter	Simulation	Experiments	References
Metabolic			
Glucose uptake[a] (kg s^{-1} m^{-3})	$1.44 \cdot 10^{-3}$	$5.4–12.6 \cdot 10^{-3}$	43
Lactate release[a] (kg s^{-1} m^{-3})	$1.35 \cdot 10^{-3}$	$5.4–9 \cdot 10^{-3}$	43
pO_2[b] (mmHg)	7	0–20	43
pH[c]	6.7	6.6–6.99	44, 45
ΔpH[d]	0.77	0.49 ± 0.08	45
Histologic			
Viable cell rim thickness[e] (μm)	155	142–310	45, 46, 47
Hypoxic rim thickness[f] (μm)	98	44 ± 52	47
Kinetic			
Cell cycle distribution			
G1 (%)	57.3	58 ± 4	48
S (%)	21.6	19 ± 1	48
G2/M (%)	21.1	23 ± 1	48

Notes: Metabolic and histologic parameters in spheroids of approximately 500 μm diameter.

[a]Rate of glucose uptake or lactate release per viable spheroid volume.

[b]Central pO_2 tension (experiments) or estimated in the centroid (simulations).

[c]pH has been determined in the central region of the spheroids. This corresponds to a sphere radius $\approx 100\,\mu$m about the centroid of the spheroid.

[d]Difference between environmental pH and pH 200 μm below the spheroid surface.

[e]In our simulations the viable cell rim thickness corresponds to the distance between the spheroid surface and the inner shell where only 5% of the cells are still alive.

[f]These values correspond to the radius of the necrotic core.

R. Chignola, A. Del Fabbro, M. Farina, E. Milotti. *J. Bioinf. Comput. Biol.* (2011) **4**: 559

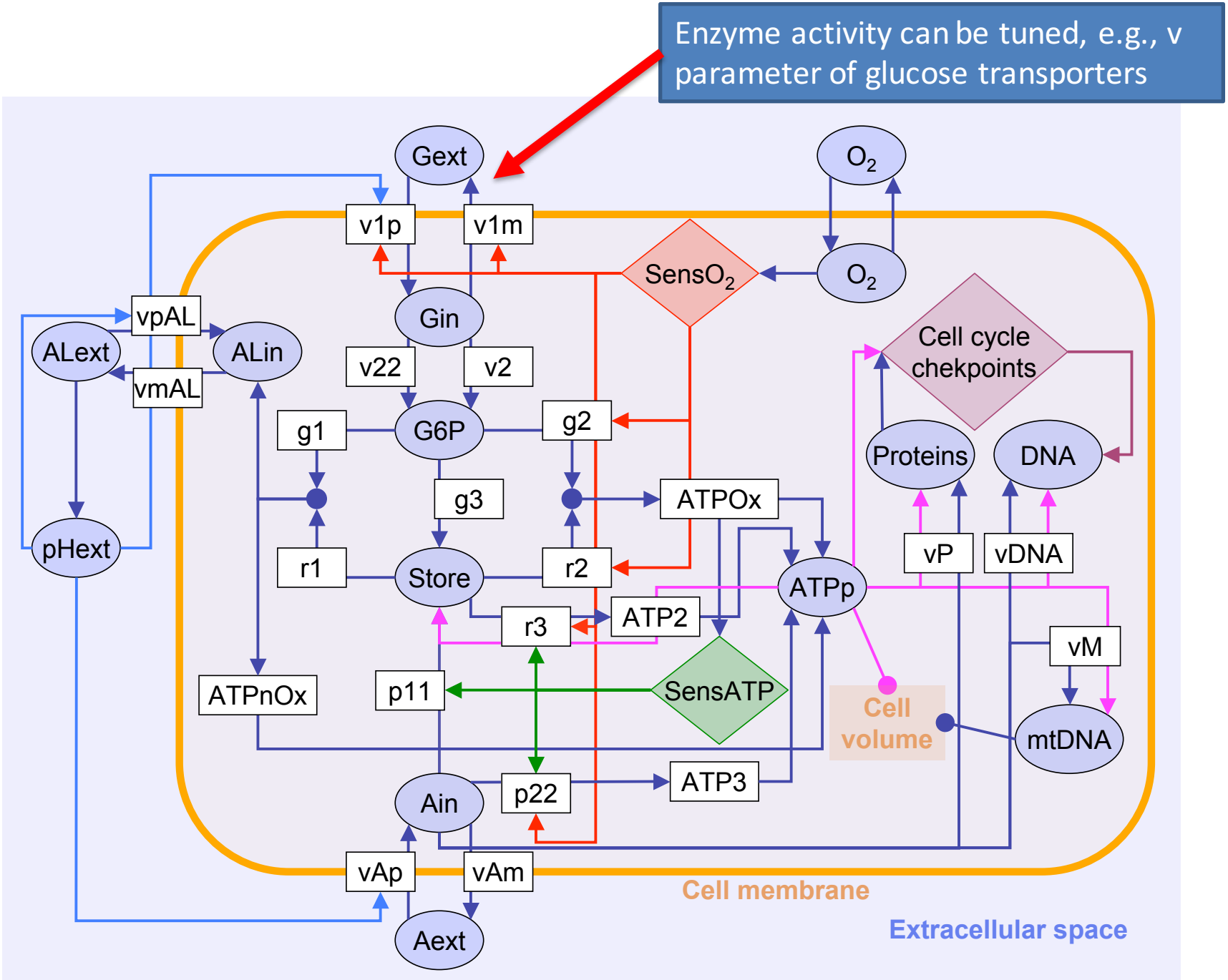
Enzyme activity can be tuned, e.g., v parameter of glucose transporters
Gext
O_2
v1p
v1m
$SensO_2$
O_2
Gin
vpAL
ALext
ALin
vmAL
v22
v2
Cell cycle chekpoints
g1
G6P
g2
Proteins
DNA
g3
ATPOx
pHext
vP
vDNA
r1
Store
r2
ATPp
r3
ATP2
vM
ATPnOx
p11
SensATP
Cell volume
mtDNA
Ain
p22
ATP3
vAp
vAm
Cell membrane
Aext
Extracellular space

The model should be changed in many ways to run in extreme enviroments, but something can be tested right away

Environmental variables:

- O2
- CO2 (*not yet implemented*)
- Glucose
- Aminoacids (glutamine)
- Lactate
- Temperature (*not yet implemented*)
- Radiation

+ time dependence of environmental variables (radiation, glucose, aminoacids)

Test runs

Simulation environment

- Dispersed cells
- Bioreactor volume: 1 cm^3
- Inflow/outflow rate: 1 cm^3/day
- Oxygen, glucose, aminoacids: standard physiological values
- Background ionizing radiation: 2.4 mSv/year

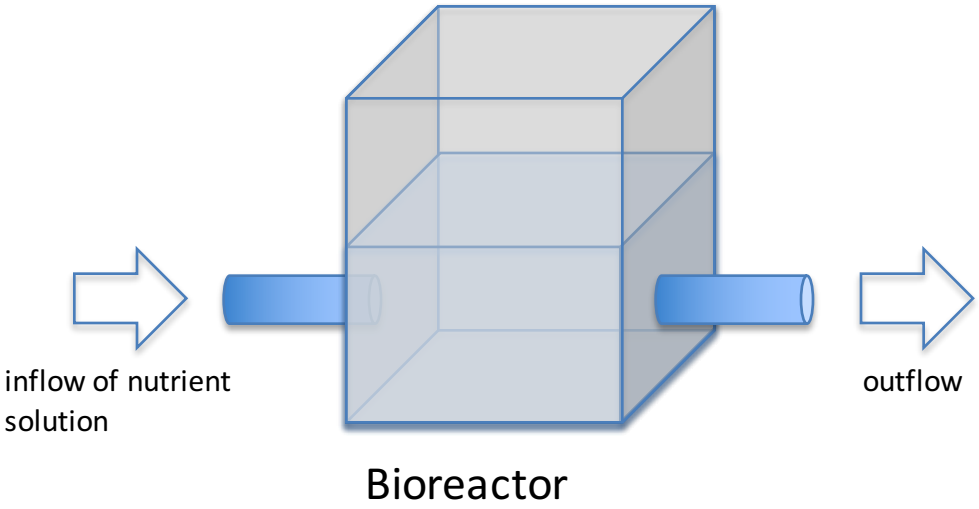

Different runs with parameters off the standard values

O2 (g/cm^3)	Glucose (g/cm^3)	Aminoacids (g/cm^3)	Lactate (g/cm^3)	pH	Background IR (Gy/s)
0	0	0	0	-	0
7.e-8	0.9e-5	0.4e-5	1.e-8	7.544	7.6e-13
14.e-8	4.5e-5	2.e-5	5.e-8	7.544	38.e-13
7.e-7	0.9e-4	0.4e-4	1.e-7	7.544	7.6e-12
14.e-7	4.5e-4	2.e-4	5.e-7	7.542	38.e-12
7.e-6	0.9e-3	0.4e-3	1.e-6	7.539	7.6e-11
14.e-6	4.5e-3	2.e-3	5.e-6	7.519	38.e-11
7.e-5	0.9e-2	0.4e-2	1.e-5	7.494	7.6e-10
14.e-5	4.5e-2	2.e-2	5.e-5	7.294	38.e-10
7.e-4	0.9e-1	0.4e-1	1.e-4	7.043	7.6e-9

Results of test runs

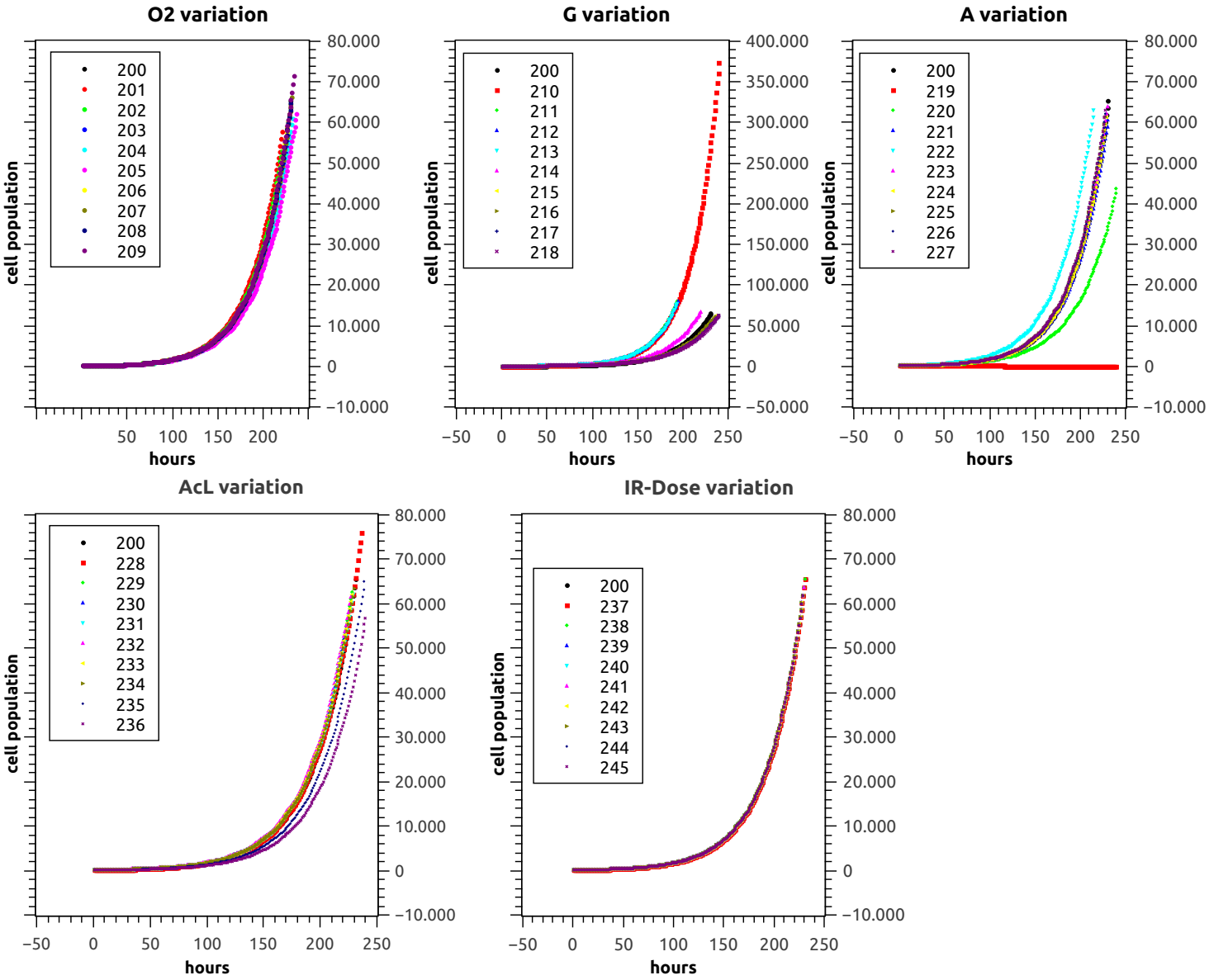

The model can be further adapted to cell life in extreme conditions

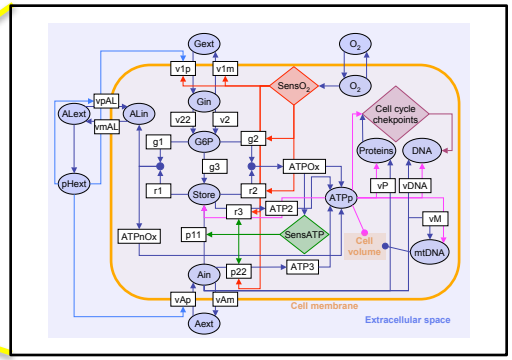

Yellowstone: the Octopus Spring where *Thermus aquaticus* was first discovered

Temperature dependence

… high-temperature environments are of especial interest, in that they reveal the extremes to which evolution has been pushed. The high-temperature environments most useful for study are those associated with volcanic activity, such as hot springs, since these natural habitats have probably existed throughout most of the time in which organisms have been evolving on earth.

T. D. Brock, "Life at High Temperatures", Science **158** (1967) 1012

It is known that eukaryotes are much less adapted to high temperatures (no eukaryote above 62 °C), while some prokaryotes live at temperatures even higher than the boiling point. Other eukaryotes are adapted to living at temperatures as low as -12 °C. Obviously this includes true metabolic life and excludes survival, like that of tardigrades in extreme environments.

We can modify the simulation program to model both low- and high-temperature eukaryotes (psychrophiles and thermophiles).
However, the algorithm would require a major overhaul to manage prokaryotes as well (still, it could be done, given enough workforce …)

Transition-state theory and temperature dependence - 1

Recall that in general

$$\Delta G = \Delta H - T\Delta S \leq 0 \quad \Rightarrow \quad \Delta H \leq T\Delta S$$

so that for a reaction

$$aA + bB \rightleftharpoons cC + dD$$

with equilibrium constant

$$\frac{[C]^c[D]^d}{[A]^a[B]^b} = \frac{k_f}{k_b} = K_{eq}$$

we find

$$K_{eq} = \exp\left(-\frac{\Delta G_0}{RT}\right)$$

Transition-state theory and temperature dependence - 2

The idea is that a better description of chemical reactions can be obtained introducing a temporary, unstable state, the transition state, as in the following example of hydrogen bond exchange:

$$H_A - H_B \quad + \quad H_C \quad \rightarrow \quad H_A - H_B - H_C \quad \rightarrow \quad H_A \quad + \quad H_B - H_C$$

transition state

The decomposition of the transition state is assumed to be the rate-determining step of the reaction

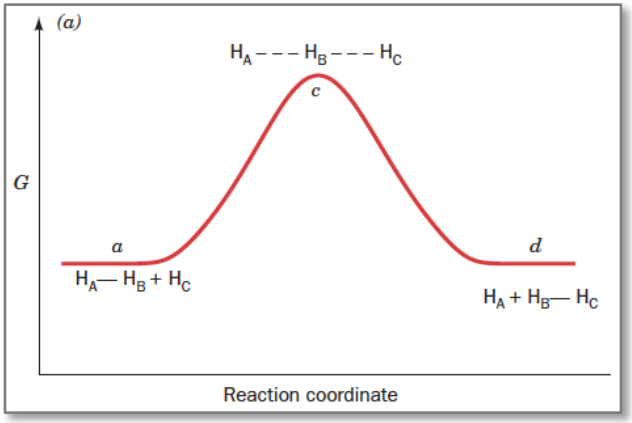

Transition-state theory and temperature dependence - 2

In general

$$A + B \underset{}{\overset{K^\dagger}{\rightleftharpoons}} X^\dagger \xrightarrow{k'} P + Q$$

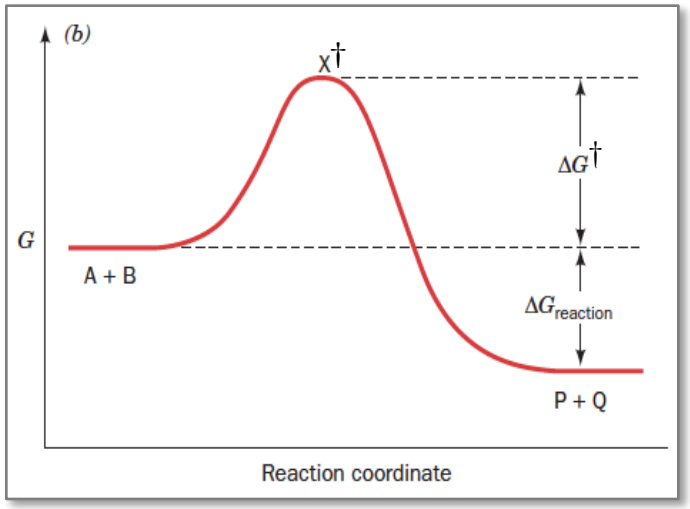

and one finds that the effective rate coefficient of the products P, Q is

$$k_{\mathrm{cat}} = \kappa \frac{k_B T}{h} \exp\left(-\frac{\Delta G^\dagger}{RT}\right)$$

Transition-state theory and temperature dependence - 4

In conventional TST enzyme activity increases with temperature, and

there is no optimal temperature, no degradation temperature

In this context the reaction is regulated by the Michaelis-Menten equation

$$V = \frac{V_{\max}[S]}{K_M + [S]}$$

with

$$V_{\max} = k_{\text{cat}}[E]_0$$

Transition-state theory and temperature dependence - 5

Enzyme inactivation can be incorporated including a temperature- and time-dependent degradation factor, so that

$$V_{\max} = k_{\mathrm{cat}}[E]_0 \exp\left(-k_{\mathrm{inact}} t\right)$$

with

$$k_{\mathrm{inact}} = \kappa' \frac{k_B T}{h} \exp\left(-\frac{\Delta G^{\dagger}_{\mathrm{inact}}}{RT}\right)$$

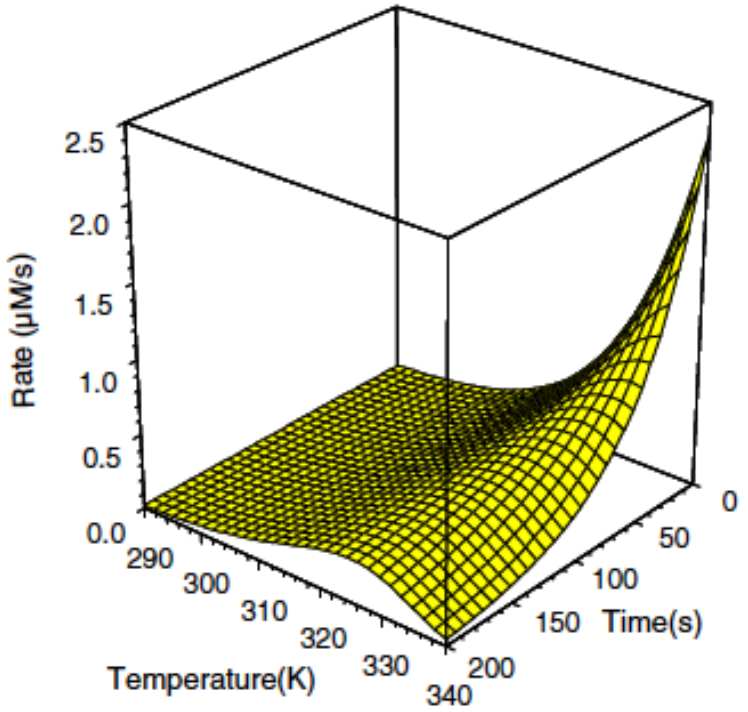

Fig. 1. The Classical theory of the effect of temperature on enzyme activity. The temperature dependence of enzyme activity with time. The data were simulated using Eqs. (2)–(4), with the parameter values: $\Delta G^{\dagger}_{cat} = 75\ \mathrm{kJ\,mol^{-1}}$ and $\Delta G^{\dagger}_{inact} = 95\ \mathrm{kJ\,mol^{-1}}$. Note that the apparent temperature optimum decreases with increasing length of the assay. Reproduced with permission from [24].

(figure from R.M. Daniel and M.J. Danson, FEBS Lett. **587** (2013) 2738)

Transition-state theory and temperature dependence - 6

In this elementary modification there is no optimal temperature at the initial time.

This problem is corrected in the "Equilibrium model" (Daniel, Danson & Eisenthal 2001), where enzymes are inactivated in a two-step process, as in TST

$$E_{\mathrm{act}} \overset{K_{\mathrm{eq}}}{\rightleftarrows} E_{\mathrm{inact}} \xrightarrow{k_{\mathrm{inact}}} X$$

then

$$V_{\max} = \frac{k_{\mathrm{cat}}[E]_0 e^{-\frac{k_{\mathrm{inact}}}{1+K_{\mathrm{eq}}}t}}{1+K_{\mathrm{eq}}}$$

with

$$K_{\mathrm{eq}} = \exp\left[\frac{\Delta H_{\mathrm{eq}}}{R}\left(\frac{1}{T_{\mathrm{eq}}} - \frac{1}{T}\right)\right] \qquad T_{\mathrm{eq}} = \frac{\Delta H_{\mathrm{eq}}}{\Delta S_{\mathrm{eq}}}$$

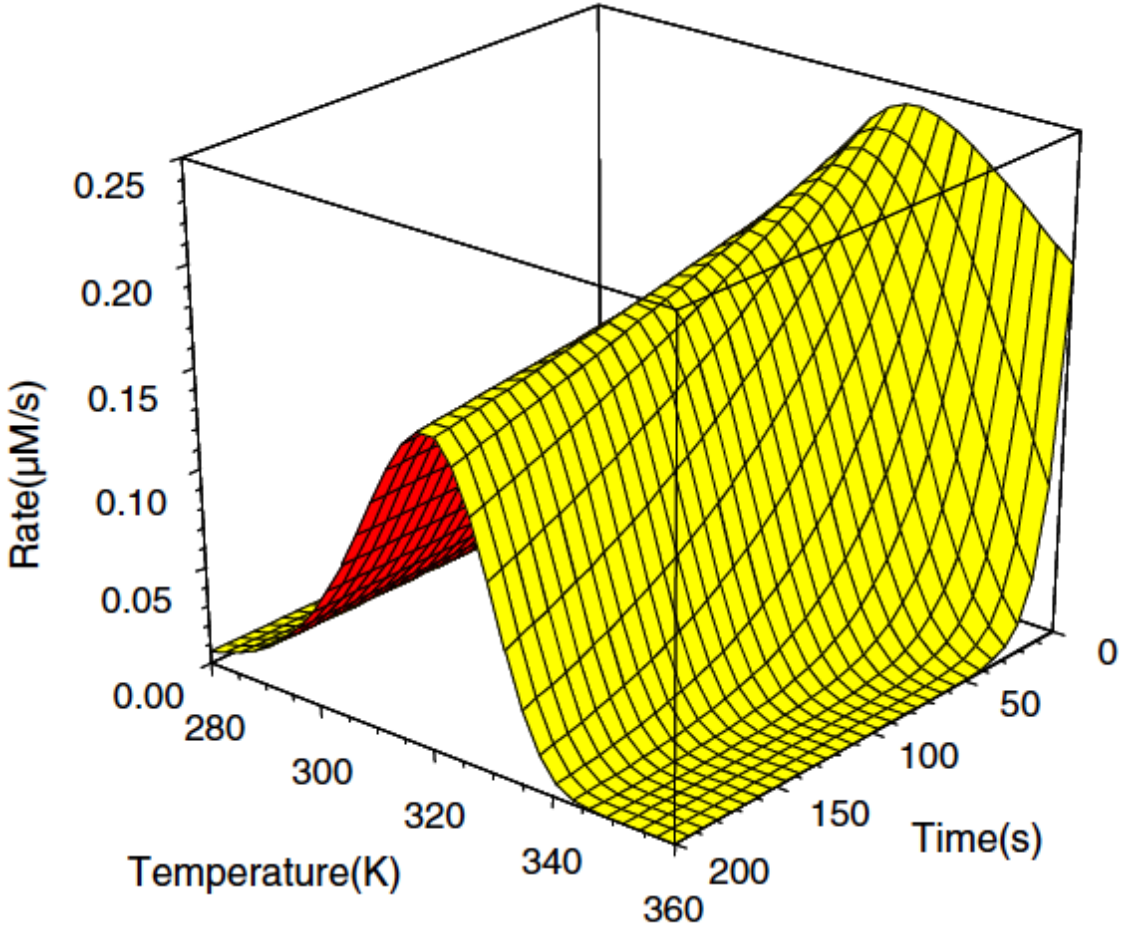

Fig. 2. The Equilibrium Model for the effect of temperature on enzyme activity. The temperature dependence of enzyme activity with time. The data were simulated using Eqs. (3)–(6), with the parameter values: $\Delta G^{\ddagger}_{cat} = 75\ kJ\ mol^{-1}$, $\Delta G^{\ddagger}_{inact} = 95\ kJ\ mol^{-1}$, $\Delta H_{eq} = kJ\ mol^{-1}$ and $T_{eq} = 320\ K$. Reproduced with permission from [24].

(figure from R.M. Daniel and M.J. Danson, FEBS Lett. **587** (2013) 2738)

Habitable zone and simulated cells

For a given simulation temperature, for a given star, and for given planetary conditions (thin or thick atmosphere, etc.), we can define a planetary distance that corresponds to that temperature.

So, if we are able to simulate the full range of temperatures where eukaryotic cells are active (-12 °C – 62 °C), we cover a range of distances from a Sun-like star

thin atmosphere: **0.58 – 0.95 AU**

earth-like atmosphere: **0.75 – 1.23 AU**

The usefulness of simulated cells lies in the ability to link the whole set of environmental conditions to cell development, and explore the fine structure of the CHZ.

pH and other adaptations of the computational model

- The simulation program already includes *parameterizations* of the pH dependence of enzyme rates. These parameterizations can be further extended to increase the reach of the model.
- The model includes a phase-dependent linear-quadratic law of cell death. This can also be further extended, e.g., with the repair-conditional repair (RCR) model
- The model can simulate small cell aggregates as well as disperse cells, and can thus model collective resistance mechanisms to environmental stress

- **All these adaptations are closely linked in the computational model, thereby providing non-trivial constraints in the definition of the CHZ.**

Conclusions

The model can be extended to provide useful information on extreme environments and on the extension of the CHZ, and can even possibly be coupled with environmental models to further improve the understanding of the interplay of biology with environment in astrobiological contexts.

This research has been carried out with the support of a grant FRA 2013 from the University of Trieste.